

RESEARCH ARTICLE

10.1029/2018JB016082

Special Section:

Magnetism in the Geosciences
- Advances and Perspectives

Key Points:

- The Burr type XII distribution is suitable as a model distribution to statistically separate the magnetic mixture in geological samples
- An automated procedure for randomly choosing initial guesses is proposed to improve the objectivity and efficiency of decomposition
- Comparing results derived from different model distributions is useful to assess the reliability of interpretations

Correspondence to:

X.Y. Zhao,
zhao.xiangyu@nipr.ac.jp

Citation:

Zhao, X.Y., Fujii, M., Suganuma, Y., Zhao, X., & Jiang, Z. (2018). Applying the Burr type XII distribution to decompose remanent magnetization curves. *Journal of Geophysical Research: Solid Earth*, 123, 8298–8311. <https://doi.org/10.1029/2018JB016082>






Received 9 MAY 2018

Accepted 23 SEP 2018

Accepted article online 27 SEP 2018

Published online 11 OCT 2018

Applying the Burr Type XII Distribution to Decompose Remanent Magnetization Curves

Xiangyu Zhao¹ , Masakazu Fujii^{1,2} , Yusuke Suganuma^{1,2} , Xiang Zhao³ , and
Zhaoxia Jiang⁴ 

¹National Institute of Polar Research, Tachikawa, Japan, ²SOKENDAI (The Graduate University for Advanced Studies), Hayama, Japan, ³Research School of Earth Sciences, Australian National University, Canberra, ACT, Australia, ⁴Key Laboratory of Submarine Geosciences and Prospecting Techniques, Ministry of Education, and College of Marine Geosciences, Ocean University of China, Qingdao, China

Abstract Discriminating magnetic minerals of different origins in natural samples is useful to reveal their associated geological and environmental processes, which can be achieved by the analysis of remanent magnetization curves. The analysis relies on the choice of the model distribution to unmix magnetic components. Three model distributions were proposed in past studies, namely, the lognormal, skew normal, and skewed generalized Gaussian distributions, which are related to the normal distribution. In this study, the Burr type XII distribution is tested and compared with existing model distributions. An automated protocol is proposed to assign parameters necessary to initiate the component analysis, which improves the efficiency and objectivity. Results show that the new model distribution exhibits similar flexibility to the skew normal and skewed generalized Gaussian distributions in approximating skewed coercivity distributions and can fit end-member components better than the commonly used lognormal distribution. We demonstrate that the component analysis is sensitive to model distribution as well as measurement noise. As a consequence, the decomposition is subject to bias that is hard to identify due to the lack of ground-truth data. It is therefore recommended to compare results derived from various model distributions to identify spurious components.

1. Introduction

Environmental magnetism has successfully demonstrated that bulk magnetic properties of natural samples are indicative of a wide range of geological and environmental processes (Evans & Heller, 2003; Liu et al., 2012). However, as natural samples usually contain a mixture of magnetic minerals, it is necessary to identify individual magnetic components in order to separate the mixed information. Several rock magnetic methods are widely used to this end, including hysteresis loop (Heslop & Roberts, 2012; von Dobeneck, 1996), magnetic susceptibility (Egli, 2009; Liu et al., 2004; Zhao & Liu, 2010), remanent magnetization curve (Egli, 2003; Heslop et al., 2002; Heslop & Dillon, 2007; Krüver et al., 2001), and first-order reversal curves (Egli et al., 2010; Roberts et al., 2000). Among them, the analysis of remanent magnetization curves, including isothermal remanent magnetization (IRM) and anhysteretic remanent magnetization curves, is the most applied technique for quantitative estimates of constituent components, known as the component analysis (see Maxbauer et al., 2016, for a summary of applications). The method assumes that the magnetization of a sample is a linear combination of contributions from constituent components, which is generally satisfied when there are negligible magnetic interactions among components (Egli, 2003). The normalized magnetization curve, $M^*(B)$, can be expressed as

$$M^*(B) = \frac{M(B)}{M_{rs}} = \sum_{i=1}^n c_i M_i(B) + \varepsilon, \quad (1)$$

where B is the magnetizing or demagnetizing field; $M(B)$ and M_{rs} are the magnetization and saturation remanent magnetization, respectively, of a bulk sample; n is the number of components; $M_i(B)$ is the normalized magnetization of the i th component with c_i being its relative contribution to the total magnetization, respectively; and ε is the residual. The component analysis can also be formulated using the first derivative of magnetization curves, that is,

$$f(B) = \frac{dM^*(B)}{dB} = \sum_{i=1}^n c_i \frac{dM_i(B)}{dB} + \frac{d\varepsilon}{dB} = \sum_{i=1}^n c_i f_i(B) + \xi. \quad (2)$$

As $f(B)$ specifies the contribution of magnetic particles to the magnetization at each coercivity interval, it is called the coercivity distribution (Egli, 2003). Note that the scale of the magnetic field (B) can be arbitrary. The most common scale is linear or logarithmic. In practice, the coercivity distribution of each component, $f_i(B)$, is in general unknown. Therefore, the essence of component analysis is to find a proper function, called the model distribution, to approximate the coercivity distribution or magnetization curve of magnetic components. Robertson and France (1994) proposed to use the lognormal distribution to model IRM acquisition curves:

$$M^*(B) = \sum_{i=1}^n c_i F_{\log n}(B; B_{1/2i}, DP_i) + \varepsilon = \sum_{i=1}^n \frac{c_i}{\sqrt{2\pi} DP_i} \int \exp\left[-\frac{(x - \mu_i)^2}{2 DP_i^2}\right] dx + \varepsilon, \quad (3)$$

where $F_{\log n}$ is the cumulative distribution function (CDF) of the lognormal distribution, $B_{1/2i}$ is the median acquisition field for the i th component where its magnetization reaches half of its saturation value, DP_i (or σ_i) is a shape factor that describes the dispersion of the distribution around its peak value, and ε is the residual. With the transformation of $x = \log(B)$, the lognormal distribution becomes the normal distribution on the logarithmic scale, where $\mu_i = \log(B_{1/2i})$. Each lognormal component is described by three parameters and is symmetrical on the logarithmic scale.

The lognormal mixture model is comprehensively studied by Kruiver et al. (2001) and Heslop et al. (2002), who also provided computer programs and hence popularized component analysis. However, it did not take long to realize the limitation of the lognormal distribution in approximating some magnetic components. For example, theoretical calculation shows that the coercivity distribution of a magnetic component can be skewed due to the presence of magnetic interaction and/or thermal relaxation (Egli, 2004b; Heslop et al., 2004), whereas the lognormal distribution is symmetrical around its mean on the logarithmic scale. In such cases, an additional lognormal component is required to fit coercivity distributions that deviate from normality. To better describe magnetic components of geological samples, generalized normal distributions have been investigated as model distributions. Egli (2003) proposed to use the skewed generalized Gaussian (SGG) distribution. The probability distribution function (PDF) is

$$SGG(x, \mu, \sigma, q, p) = \frac{1}{2^{1+\frac{1}{p}} \sigma \Gamma\left(1 + \frac{1}{p}\right)} \frac{|q e^{qx^*} + q^{-1} e^{x^*/q}|}{e^{qx^*} + e^{x^*/q}} \exp\left[-\frac{1}{2} \left|\ln\left(\frac{e^{qx^*} + e^{x^*/q}}{2}\right)\right|^p\right], \quad (4)$$

with $x^* = (x - \mu)/\sigma$, $\sigma > 0$, $0 < |q| \leq 1$, and $p > 0$, x is the logarithmic magnetic field instead of the linear field (B), that is, $x = \log_{10} B$. The shape of an SGG component is controlled by four parameters, which are the location (μ), dispersion (σ) as in the normal distribution, and two additional parameters that modulate the skewness (q) and kurtosis (p). The SGG distribution can cover a wide range of shapes including skewed ($|q| \neq 1$), peaked ($p < 1$), and squared ($p \gg 2$) shapes due to these two additional parameters. The normal distribution is a special case of the SGG distribution with $q = 1$ and $p = 2$ (Egli, 2003). A broad spectrum of geological samples was analyzed comprehensively using the SGG distribution. Representative components are identified and classified as detrital, biogenic, pedogenic, urban pollution, dust components, and so on (Egli, 2004a, 2004c, 2004b). Skewness plays a more important role than kurtosis in modeling geological samples as most components are characterized with p close to 2 (Egli, 2004a). As a simplification, Maxbauer et al. (2016) applied the skew normal distribution and found that resulting components using the skew normal distribution are comparable to those based on normal and SGG distributions.

In principle, model distributions should closely represent the coercivity distribution of end-member magnetic components in order to get reliable results. However, data of end-member magnetic components are rare as it is often impossible to physically extract individual components from natural samples. Moreover, it remains challenging to faithfully model coercivity distributions of natural components given the complex nature of coercivity. Hence, the choice of model distributions is empirical. As the SGG distribution can cover an extremely wide range of skewness and kurtosis, it is a versatile model distribution when a priori information about the constituent components is unknown, and is considered as the gold standard for magnetic component analysis (Heslop, 2015). Nevertheless, since ground-truth data are unavailable, it remains problematic to verify how faithful the reconstructed components are. For this matter, it would be helpful to have other flexible model distributions for comparison in order to judge the sensitivity of results to the choice of model distributions, but there is few option since distributions other than generalized normal distributions have been overlooked.

Regardless of model distributions utilized, component analysis is known to be sensitive to measurement noise (Egli, 2003). It is not guaranteed that correct estimates of parameters can be obtained in the presence of noise. Moreover, it is practice to convert raw data to the first derivative for component analysis, which amplifies the measurement noise (Heslop, 2015). Though methods such as spline interpolation (Heslop et al., 2002; Maxbauer et al., 2016), low-pass filtering, and linearization of measurement (Egli, 2003) have been proposed to reduce the noise in the original data, it is unclear how well the signal can be separated from noise. If component analysis can be based on the cumulative form of the mixture model as in equation (1), the analysis should be less affected by noise as it avoids the amplification of noise. However, only the component analysis tool (IRM-CLG) published by Kruiver et al. (2001) is based on the cumulative lognormal distribution. The cumulative form is less popular since probability distributions usually do not have closed-form mathematical expressions for CDFs. For example, the computation of the CDF of the SGG distribution requires customized code for numerical integration, which will significantly slow down the analysis and thus hinder the application using its CDF form. As a result, the performance of the CDF form of the mixture model on the one hand and the performance of the PDF form on the other hand are little compared.

The Burr type XII distribution is a generalized log-logistic function, and one of its limiting case is the Weibull distribution (Rodriguez, 1977). It covers a rich range of skewness and kurtosis that overlaps with many other distributions (Rodriguez, 1977). Furthermore, the CDF of the Burr type XII distribution has a closed-form mathematical expression. In this paper, we will examine the suitability of the Burr type XII distribution as a model distribution. Both CDF and PDF forms of the mixture model using the Burr type XII distribution are applied to noisy data in order to compare their sensitivity to noise. We also perform component analysis on synthetic and natural samples to compare performances of the lognormal, SGG, and Burr type XII distributions, followed by the discussion of the roles of model distributions and measurement noise in component analysis.

2. The Burr Type XII Distribution and Methods

Burr (1942) introduced a system of distributions with the purpose of fitting a CDF to data rather than fitting a PDF to the derivative of data. The type XII distribution is one of the 12 distributions in the system and is the one that was extensively studied by Burr (1942). For component analysis, we adopt a three-parameter form for the CDF and PDF (Tadikamalla, 1980):

$$F_{\text{Burr}}(B; \alpha, \gamma, \lambda) = 1 - \left(1 + \left(\frac{B}{\lambda}\right)^{\gamma}\right)^{-\alpha}, \alpha > 0, \gamma > 0, \lambda > 0, \quad (5)$$

and

$$f_{\text{Burr}}(B; \alpha, \gamma, \lambda) = \frac{\alpha\gamma}{\lambda} \left(\frac{B}{\lambda}\right)^{\gamma-1} \left(1 + \left(\frac{B}{\lambda}\right)^{\gamma}\right)^{-\alpha-1}, \alpha > 0, \gamma > 0, \lambda > 0, \quad (6)$$

respectively, where B is the linear magnetic field, λ is the scale parameter that adjusts the width of distribution, and the shape is modulated by α and γ . The distribution is unimodal when $\gamma > 1$, and narrows down as α and/or λ increase. Detailed information of the variability in shape can be found in Burr (1942), who provided a table and a graph of skewness as a function of shape parameters. In order to compare with the SGG distribution, the Burr type XII distribution is transformed to a logarithmic scale, which also changes the skewness and kurtosis accordingly, but the flexibility in shape is not compromised. For example, the Burr type XII distribution becomes the logistic distribution (which is the log-logistic distribution on the linear scale) when $\alpha = 1$, which is symmetrical and similar to the normal distribution except that it has slightly heavier tails as shown in Figure 1a. Note that only in this case is λ equal to the median acquisition field as $F_{\text{Burr}}(B = \lambda; \alpha = 1) = 0.5$. Examples of asymmetric Burr type XII distributions are shown in Figure 1b.

The Burr type XII distribution can approximate the individual magnetic components that are identified and modeled using the SGG distribution (Egli, 2004a). Figure 2a shows examples of magnetic components modeled by the SGG distribution (gray curves; Egli, 2004a) in comparison with their best fits using the Burr type XII distribution (colored curves). The corresponding residuals have sinusoidal shape (Figure 2b). Similarly, the Burr type XII distributions can also be closely fitted by the SGG distribution (Figure 2c) with even smaller residuals (Figure 2d).

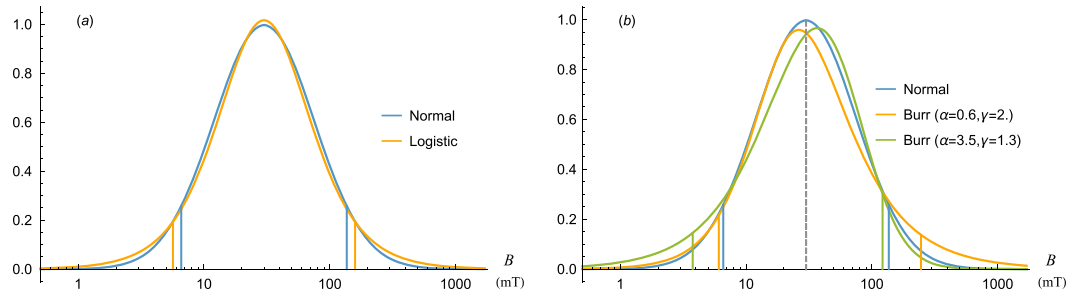


Figure 1. Examples of the Burr type XII distribution on the logarithmic scale. (a) A symmetric Burr type XII distribution ($\alpha = 1$), that is, a logistic distribution, is similar to the normal distribution except for heavier tails. (b) Skewed Burr type XII distributions versus a normal distribution. All distributions have the same median value (indicated by the dashed vertical line). The vertical bars indicate the 5th and 95th percentiles of corresponding distributions.

When using the Burr type XII distribution as the model distribution, the mixture model in the CDF form can be expressed as

$$M(B) = \sum_{i=1}^n c_i F_{\text{Burr}}(B; \alpha_i, \gamma_i, \lambda_i) + \varepsilon. \quad (7)$$

Or it can be expressed in the PDF form on the logarithmic scale

$$\frac{dM(x)}{dx} = \ln 10 \sum_{i=1}^n c_i f_{\text{Burr}}(10^x; \alpha_i, \gamma_i, \lambda_i) 10^x + \frac{d\varepsilon}{dx} \quad (8)$$

where $x = \log_{10} B$. Each component is described by four parameters, that is, contribution (c_i), the scale parameter (λ_i), and shape factors (α_i and γ_i). If the magnetization curve reaches the saturation, there is $\sum_{i=1}^n c_i = 1$ for the normalized curve. In this case, c_n can be simply set equal to $1 - \sum_{i=1}^{n-1} c_i$, and the number of free parameters for n components is $4n - 1$. The parameters are estimated using nonlinear least squares regression.

For component analysis, it is necessary to choose the number of components and their initial parameters to initiate the nonlinear regression. They are usually provided by users in a trial-and-error manner. This manual

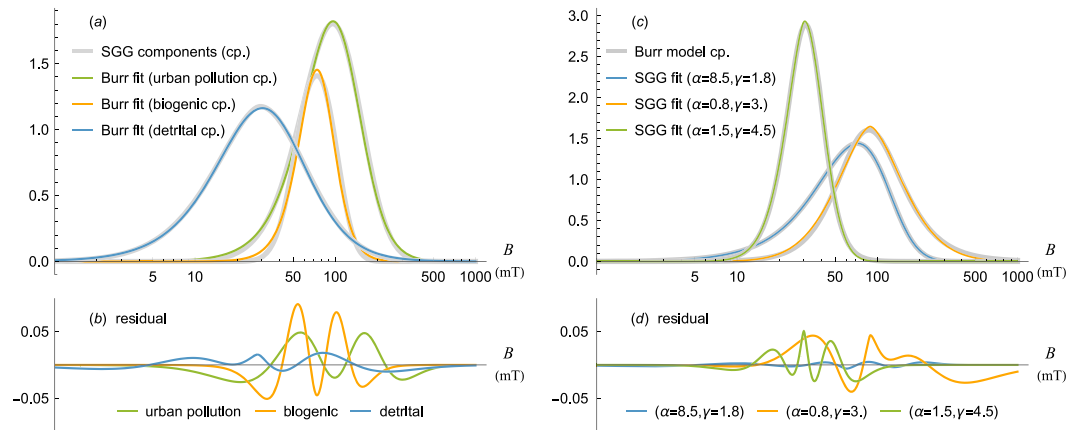


Figure 2. Comparison between the Burr type XII distribution and the skewed generalized Gaussian (SGG) distribution. (a) The SGG components (gray lines, from Egli (2004a)) and best fits of the Burr type XII distributions (colored lines) with the following shape parameters (α, γ): detrital cp ($\alpha = 1.517, \gamma = 1.806$), biogenic cp ($\alpha = 1.446, \gamma = 4.568$), and urban pollution cp ($\alpha = 2.055, \gamma = 2.657$). (b) Corresponding residuals. (c) Best fits of the SGG distribution (colored lines) to the modeled Burr components (gray lines). Shape parameters for modeled components are shown in legends. (d) Corresponding residuals. Note that cp means component.

step makes component analysis not only inefficient but also sensitive to users' choices. As an improvement, we make these procedures automatic by using the following two protocols for choosing initial parameters and the optimal number of components.

2.1. Choice of Initial Guesses for Parameters

In general, nonlinear least squares regression cannot guarantee that the global minimum is reached since it is likely to reach to local minima depending on initial guesses. Except for the IRM UnMix program (Heslop et al., 2002), all programs require users to manually provide initial guesses to start an analysis. However, as it is not intuitive to come up with initial guesses that lead to global minimum, users have to adjust all parameters in a trial-and-error manner (Heslop, 2015). In fact, this procedure can be done automatically. For this purpose, the range of each parameter needs to be constrained. For the Burr type XII distribution, the contribution parameter varies between 0 and 1. The bounds for shape parameters (α and γ) can be predefined based on general observation. For example, extreme values of α and γ will result in unrealistically wide (as $\alpha, \gamma \rightarrow 0$) or narrow (as $\alpha, \gamma \rightarrow \infty$) coercivity distributions. Therefore, α and γ can be constrained to [0.4, 16] and [0.5, 16], respectively, in the program. Note that though the distribution is unimodal on a linear scale when $\gamma > 1$, it can be unimodal on a logarithmic scale with $\gamma \leq 1$, depending on the value of α . Though $\lambda \neq B_{1/2}$, in general, the ratio, $r = \lambda/B_{1/2}$, is a function of α and γ , which increases with increasing α and decreasing γ . Since $B_{1/2}$ for most natural magnetic minerals is well below 2 Tesla, we have $\lambda < 2r$ Tesla. Within the above ranges of α and γ , r reaches maximum (510.16) with $\alpha = 16$ and $\gamma = 0.5$, but this value is too large to be a useful constraint. In fact, r decreases sharply as γ increases, for example, $r \approx 22.6$ with ($\alpha = 16, \gamma = 1.0$) and $r \approx 8$ with ($\alpha = 16, \gamma = 1.5$). Therefore, from the practical standpoint, λ can be set to range between (0, 16] Tesla. Given the number of components, initial values can then be randomly drawn from within the given bounds. With each set of sampled parameters, the program fits the data and records the residual sum of squares (RSS). This procedure will repeat for a given number of times (e.g., $n = 20$), and the result with the smallest RSS will be chosen. Note that the analysis may result in components with negative c_i . Such results will be discarded automatically. This protocol exempts users from the effort of providing initial guesses, improving the efficiency as well as the objectivity of the analysis.

2.2. Model Selection

Excessive number of components provides better fitting yet misleading results. It is therefore critical to determine the appropriate number of components. The Akaike information criterion (AIC) provides a means of model selection by quantifying the trade-off between the goodness of fit of the model and the number of the parameters of the model (Akaike, 1998). The AIC is defined as the difference between the number of parameters and the maximum value of the likelihood function for the model. As we use a least squares method, the maximum value of the likelihood function is equivalent to the RSS of the fitting given the assumption that the noise is normally distributed (Burnham & Anderson, 2002), and the AIC is expressed as follows:

$$AIC = 2k + N \ln \sum_{i=1}^N \left(y_i - f(x_i; \hat{\theta}) \right)^2 + C = 2k + N \ln RSS + C, \quad (9)$$

where k is the number of parameters (θ), $\hat{\theta}$ is the best fit estimates of θ , N is the number of data points, and C is a constant. As a smaller AIC score is favored, the term of $2k$, which is positive, penalizes the increase in the number of components. AIC scores as a function of N can be calculated, and the number of components that gives the minimum AIC score will be used as the optimal value for further analyses.

3. Results

In this section, we demonstrate the results of component analysis using the Burr type XII distribution as well as the lognormal and SGG distributions. Since all results are shown on the logarithmic scale for comparison, the lognormal distribution is indicated as the normal distribution. The components in the following examples are widely overlapping, which are difficult to recover (Egli, 2003). The first two parts test noise-free and noisy data, respectively. The third part compares the model distributions by applying them to experimental data.

Table 1
Parameters for the Modeled Components and the Best Fits Shown in Figure 3

Case	cp ^a	Model parameters				Best fits			
		c	λ (mT)	α	γ	c	λ (mT)	α	γ
A	#1	0.32	50	1.0	2.0	0.320	49.991	1.000	1.999
	#2	0.68	25	2.0	1.2	0.680	25.014	2.003	1.500
B	#1	0.15	100	2.0	3.3	0.150	99.963	1.999	3.299
	#2	0.40	40	1.0	3.0	0.400	40.010	1.001	3.000
	#3	0.45	25	1.5	1.5	0.450	24.991	1.498	1.500

^acp: component.

3.1. Noise-Free Modeled Data of the Burr Type XII Distribution

Cases A and B are composed of two and three components, respectively. The model parameters and their estimates are listed in Table 1. In each case, there are 60 data points that are evenly distributed on the logarithmic scale. The fitting uses the CDF form of the mixture model, and the results are shown as coercivity distributions as it is more informative. In Case A, the two constituent components have largely overlapping coercivity spectra with distinct median coercivity. In the case of two components, it is easy to obtain close estimates even with default initial guesses for each parameter (Figure 3a). For a unimodal distribution with three components (case B), default initial guesses may lead to wrong estimates even though

noise is absent (not shown). In such cases, the automatic approach for choosing initial guesses (see section 2.1) becomes helpful to get better estimates (Figure 3b).

3.2. Noisy Modeled Data of the Burr Type XII Distribution

As noise is always present in real data, it is important to test the effect of noise on component analysis. The noise is modeled as a Gaussian white noise, $n(B) = a * w(B; \sigma^2 = 1)$, where B is the magnetic field, a is the amplitude, and σ^2 is the variance of the noise. Noise is added to the modeled data shown in Figure 3a. To test the sensitivity of component analysis to noise, the analyses are performed on the same data using both the CDF and PDF forms of the mixture model. To avoid the potential effect of initial guesses, identical initial guesses are used in both cases. Figure 4a shows the result based on the CDF mixture model (but the gradient curve is shown instead). With a minor noise ($a = 0.0002$), the estimated components are slightly different from the modeled components. The sum of estimated components is close to the data though (Figure 4a), which can also be seen in Figure 4b where the residual of the best fit (black) approximates the noise (gray) with a small difference (blue) that has a low-frequency feature. Note that in Figure 4b it is the noise in the original data (M) that is shown not that in the gradient curve ($dM/d\log B$). On the other hand, the result based on the PDF mixture model is biased to a greater extent (Figure 4c). There are two reasons. First, the fitting is performed on the gradient curve where the noise level is enhanced by a factor of 10 by differentiation (Figure 4d). If we increase the noise added to the original signal by a factor of 10, the result using the CDF mixture model will be similarly biased (not shown). It suggests that the CDF form of mixture model should be preferred over the PDF form in order to avoid amplifying measurement noise. Second, the shape of noise profile is changed by differentiation. As an example, Figure 4e shows the result of component analysis on the data of the same components with a different noise profile (Figure 4f). Though the noise profiles shown in Figures 4b and 4f have the same amplitude ($a = 0.0002$), their impact on the result is different.

It is more difficult to get close estimates from noisy data as the number of components increase. Figure 4g shows the result for a case with three components. The noise profile in this example is the same as that shown in Figure 4b. The contribution of the first modeled component (orange) is set to 15% and the estimate is 20.0%, which is 33% off the true value. The estimated contribution of the second component (green) is ~18% off. If the noise is doubled in amplitude, the bias becomes even worse with the estimated concentration of the first component being almost 2 times its true value (not shown).

Table 2
Parameters for the Modeled Components and the Best Fits Shown in Figure 4

Case	cp	Model parameters				Best fits			
		c	λ (mT)	α	γ	c	λ (mT)	α	γ
A (Figure 4a)	#1	0.32	50	1.0	2.0	0.361	50.032	1.023	1.956
	#2	0.68	25	2.0	1.2	0.639	28.054	2.419	1.197
A (Figure 4c)	#1	0.32	50	1.0	2.0	0.453	49.133	1.110	1.871
	#2	0.68	25	2.0	1.2	0.548	39.681	4.153	1.189
B (Figure 4g)	#1	0.15	100	2.0	3.3	0.200	93.753	1.752	3.238
	#2	0.40	40	1.0	3.0	0.326	44.460	1.513	2.972
	#3	0.45	25	1.5	1.5	0.475	24.785	1.392	1.497

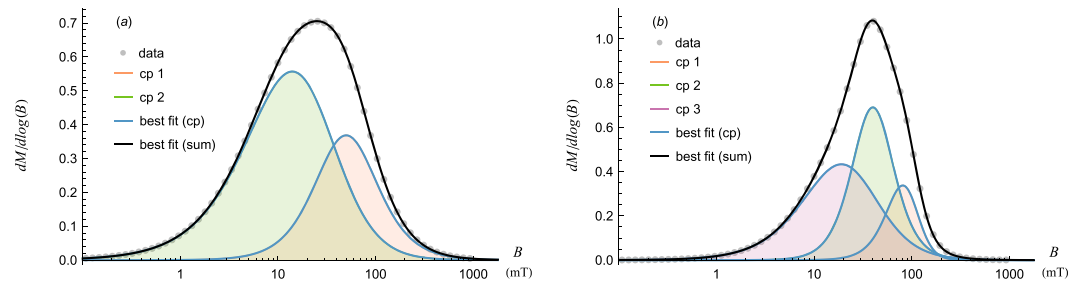


Figure 3. Component analysis of noise-free modeled data. (a) The modeled data (dots) consist of 2 Burr type XII components whose coercivity distributions are indicated by the colored areas. The estimated components are shown in blue lines, and the total distribution is in black. (b) The case with three modeled components. Parameters are shown in Table 1.

3.3. Modeled Data of Other Distributions

As shown above, noise has a significant effect on component analysis using the mixture model of the Burr type XII distribution. In this part, we examine mixture models using the normal and SGG distributions for comparison. As the normal distribution is a special case of the SGG distribution, the same noisy modeled data, consisting of two normal components, is used for test. The noise level is the same as

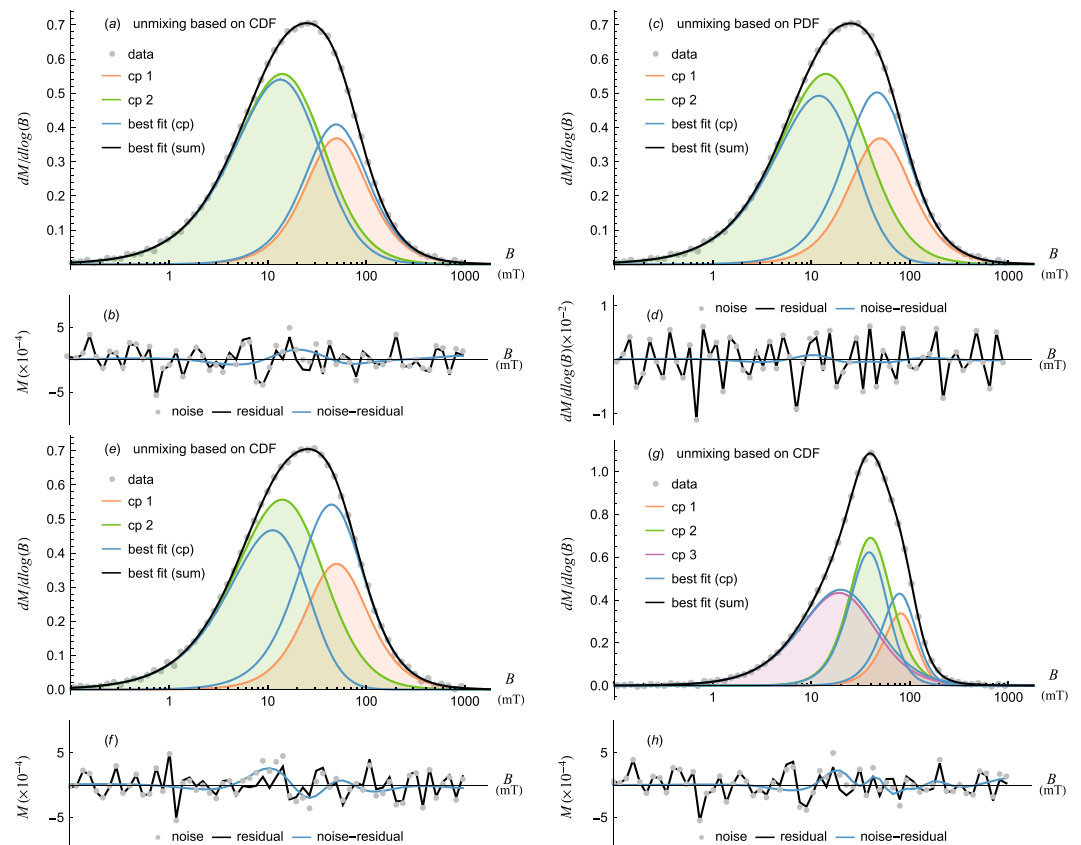


Figure 4. The component analysis of noisy data. (a) The modeled data (dots) consist of two Burr type XII components (cp1 and cp2, shown as green and orange curves) and noise. The estimated components and the sum are shown in blue and black lines, respectively. Note that the analysis is based on the cumulative form of the mixture model. (b) The residual of the analysis (black) versus the modeled noise (dots). The blue line indicates the difference between the residual and modeled noise. (c and d) Same as (a) and (b) except that the analysis is performed on the coercivity distribution using the probability distribution function (PDF) form of the mixture model. (e and f) Same as (a) and (b) except that the modeled noise is different. (g and h) The case with 3 modeled components. The modeled noise is the same as that used in (a). Parameters of best fits are listed in Table 2.

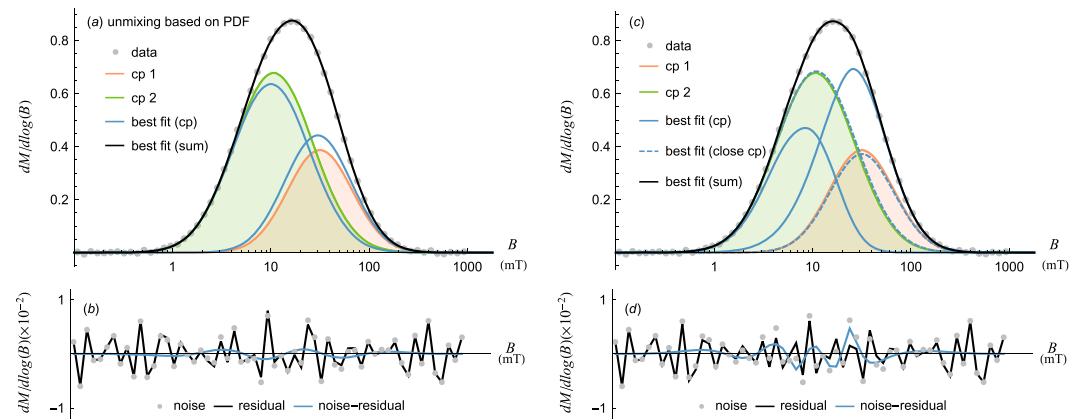


Figure 5. Component analysis using the normal and skewed generalized Gaussian distributions. (a) The modeled data (dots) consist of two normal components (cp1 and cp2, shown as green and orange curves) and noise. The best fit components and the sum are shown in blue and black lines, respectively. (b) The residual (black) versus the modeled noise (dots). The blue line indicates the difference between the residual and the noise. (c) Results based on the SGG distribution. The data are the same as that shown in (a). The solid blue lines and dashed lines indicate results with two different sets of initial guesses. (d) The residual (black) corresponds to the results shown in solid blue lines in (c).

above cases ($\alpha = 0.0002$). Similar to previous cases, the results are affected by noise (Figure 5). The normal mixture model is relatively stable in the sense that the results based on PDF and CDF mixture models are similar to each other and both are close to the true values (Figure 5a, using the PDF mixture model). One reason is that the normal distribution involves fewer parameters. In contrast, when using the SGG mixture model with the same initial guesses where contribution parameters for the two components are set to 0.5, the estimate is apparently wrong (estimated components are shown in solid blue lines in Figure 5c, and the corresponding residual is shown in Figure 5d together with the modeled noise). However, if the initial guesses of the contribution are tuned to be closer to the true values, the SGG model can result in a very good estimate (dashed lines in Figure 5c) in this case. However, the fitting that gives a *correct* estimate in fact has a larger RSS ($5.45E-4$) than that of the *wrong* estimate ($4.88E-4$). This example suggests that the global minimum of the object function that the nonlinear regression method optimizes is shifted by the noise away from its *true* position, which is the main reason that the component analysis is sensitive to noise.

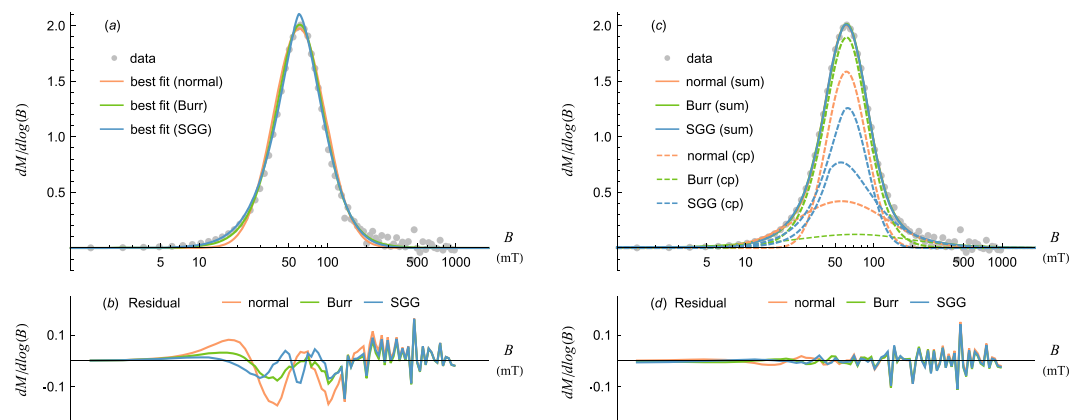


Figure 6. Component analysis of synthetic magnetite. (a) Results of component analysis using a single component. The raw data are shown as dots. The best fits of the normal, Burr type XII, and SGG distributions are shown in orange, green, and blue curves, respectively. The Burr component is characterized with $\alpha = 1.085$, $\gamma = 3.407$ and $\lambda = 62.293$ mT. (b) Residuals. (c) Results of component analysis using two components. Color codes are the same as in (a). Individual components are shown as dashed lines. Sums are shown as solid lines. (d) Residuals.

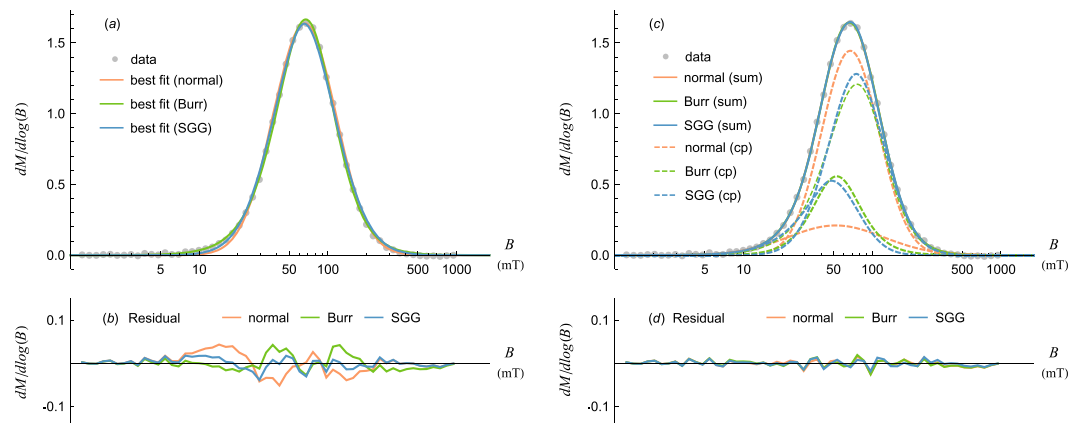


Figure 7. Component analysis of serpentinized peridotite. (a) Results of component analysis using a single component. The raw data are shown as dots. The best fits of the normal, Burr type XII and SGG distributions are shown in orange, green, and blue curves, respectively. The parameters for the Burr component are $\alpha = 1.244$, $\gamma = 2.721$, $\lambda = 72.872$ mT. (b) Residuals. (c) Results of component analysis using two components. Color codes are the same as in (a). individual components are shown as dashed lines. The sums are shown as solid lines. (d) Residuals.

3.4. Component Analysis of Experimental Data

In previous examples, the modeled data are based on the same distribution as the mixture model. In practice, however, the coercivity distribution of constituent components is in general unknown. Analysis may have different results depending on the choice of model distributions. Therefore, it is useful to compare different model distributions in order to judge if the estimated components are reliable, as illustrated by the following examples. First, we chose a sample of synthetic magnetite, which is produced by reducing hematite at 395 °C in a mixed gas (80% CO₂ and 20% CO) for 72 hr. The detail of the sample is given by Jiang et al. (2016) (the sample ID therein is I-4.). The IRM acquisition curve was measured up to a maximum field of 1 T on a vibrating sample magnetometer (MicroMag™ VSM 3900). As the magnetite is made in a single process, it is expected to have one single component. The normal distribution can approximate the data with one component (Figure 6a) but with noticeable residuals especially in the left tail (Figure 6b). On the other hand, the Burr type XII and the SGG distributions can better fit the data with a single component (Figures 6a and 6b). Using two components, the overall fits are improved for all model distributions (Figures 6c and 6d). The estimated components, however, are not consistent at all (Figure 6c). The comparison suggests that the results with two components are spurious though they are associated with better AIC scores and smaller residuals. In fact, the sine-wave like residuals in Figure 6b are similar to the pattern shown in Figures 2b and 2d. Therefore, it suggests that the residual is due to the fact that the model distributions are different from the actual coercivity distribution of the sample, rather than under-fitting.

The second example is a serpentinized peridotite sampled from the Yokoniwa Rise, Central Indian Ridge (Fujii et al., 2016). The peridotites investigated by Fujii et al. (2016) had experienced different degrees of serpentinization due to hydrothermal reaction. Here we chose the sample (ID: 6k#1170R12) with a 96% serpentinization as an end-member. Its detailed rock magnetic properties are listed in Fujii et al. (2016). The IRM acquisition curve was measured on an alternative gradient magnetometer (MicroMag™ AGM 2900) hosted in the National Institute of Polar Research, Japan. The coercivity distribution of the rock sample is similar to that of the synthetic magnetite shown in Figure 6. With a single component, all the three model distributions can fit the data closely except that the normal distribution results in larger residuals in the left tail (Figures 7a and 7b). With two components, the fits are all improved and the residuals for all distributions become almost identical as shown in Figure 7d. AIC scores also suggest that the optimal number of components is 2. Moreover, the components based on the SGG and Burr type XII distributions are very similar for this sample (blue and green dashed lines in Figure 7c). Unlike the case shown in Figure 6b, the consistency between different mixture models is excellent, which implies that the interpretation of two components is also plausible. In fact, the microscopic observation shows that the texture of the rock sample and the morphology of magnetic particles therein are highly heterogeneous. For example, the rock contains porous micron-sized magnetite in the matrix as well as submicron magnetite grown in developed veins (Figures 2 and 5 in Fujii et al.,

2016). Therefore, magnetite particles in the sample could be formed by different processes and thus have different coercivity distributions. It requires further information or knowledge to verify the interpretations for this sample.

4. Discussion

In this part, we first compare the model distributions against coercivity distributions of end-member magnetic components. Then, critical problems associated with unmixing components are addressed in order to better understand component analysis, followed by discussion of precautions and possible solutions.

4.1. Comparing Model Distributions as End-Member Coercivity Distributions

The lognormal distribution was the first and most commonly used model distribution for magnetic component analysis. It has fewer parameters than other distributions and is more resistant to noise. However, it may not closely represent the coercivity distribution of magnetic components of geological samples due to its fixed symmetry. Theoretical calculation shows that a single magnetic component tends to have a left-skewed coercivity distribution (i.e., negative skewness) due to factors such as physical properties (e.g., grain size, elongation of particles, and defects of the crystal structure) and thermal activation (Egli, 2004b). In order to fit a skewed coercivity distribution using the lognormal distribution, additional components will be required in order to fit the low and/or high ends of the coercivity distribution. In contrast, the skew normal and SGG distributions, which have flexible skewness (Egli, 2003; Maxbauer et al., 2016), can better handle such situations (see Figures 6a and 7a for example). Though the SGG distribution covers an extremely wide range of skewness and kurtosis, when applied to natural and synthetic samples (Egli, 2004a, 2004b, 2004c), most magnetic components are characterized with a moderate negative skewness (Egli, 2003; Egli, 2004a). As the default parameter space of the SGG distribution is excessive for natural samples, it makes the analysis more subject to nonuniqueness (see section 4.2). Furthermore, a SGG component may effectively approximate a combination of two lognormal components, as shown in Figure 10 in Egli (2003). In such situations where coercivity distributions of two components overlap considerably, using the SGG distribution might underestimate the number of underlying components, which is a general problem when using complicated model distributions (Egli, 2003). While narrowing the parameter space is helpful for this problem, it is also important to have other model distributions for comparison in order to identify spurious results. Compared to the SGG distribution, the Burr type XII distribution has a moderate shape variability. It can approximate end-members of the natural components reconstructed using the SGG distribution (Figure 2a). When applied to experimental data of end-members, the SGG and Burr type XII distributions can fit data similarly well with a single component as shown in Figures 6a and 7a. These examples suggest that the Burr type XII distribution is a promising alternative model distribution for natural end-member components. For future work, it is worth investigating more natural end-members using different model distributions to justify if they are qualified.

4.2. Nonuniqueness of Component Analysis

When analyzing samples consisting of several magnetic components, there can be multiple solutions, corresponding to local minima of the object function. With different initial guesses, the nonlinear regression will tend to end up in different minima, causing the well-known nonuniqueness problem. This problem is more prominent for the Burr type XII and SGG distributions than for the normal distribution. For example, the mixture model of SGG distributions is more sensitive to initial guesses than that of normal distributions, as shown in Figure 5c, because of its highly flexible nature. In fact, a part of SGG distributions, such as peaked and squared curves, is unrealistic for natural or synthetic samples. It means the parameter space is much wider than necessary for component analysis. For this reason, narrowing the parameter space would be helpful to reduce the nonuniqueness of component analysis in general (Maxbauer et al., 2016). For this purpose, Egli (2003) suggested that the natural components can be modeled with $|q| > 0.5$ and $1.6 < p < 2.5$. Furthermore, Egli (2004b) related the kurtosis parameter (p) with skewness parameter (q) by $p(q) \approx 2 + (1 - q)^5$ based on information theory and a wide collection of experimental data. In this case, p is close to 2 and dependent on q . Hence, the number of independent parameter is reduced to 3 for a SGG magnetic component. We applied the original and the simplified SGG distribution to fit the data of sample I-4. The original SGG component in Figure 6a shows a pronounced and unnatural peak that is not featured by the measured data. This peak is possibly an artifact due to the relative high noise level in the right tail. With the simplified SGG model, we can get a solution that better fits the peak. However, due to the restriction on the parameter

space, the overall fitting is not as good as the original one and the resulting RSS is similar to that of the single lognormal component. If $p(q) \approx 1.75 + (1 - q)^5$ is applied, the result is improved compared to that with $p \approx 2$. It suggests that the optimal relationship of p and q may be subject to change.

Due to the nonuniqueness problem, the choice of initial guesses becomes nontrivial in many cases. Most of the published component analysis tools (Egli, 2003; Kruiver et al., 2001; Maxbauer et al., 2016) require users to test several sets of initial guesses for individual samples to obtain the best fit. The interactive user interface designed by Maxbauer et al. (2016) is helpful for users to come up with meaningful guesses, but it is still inefficient especially for multiple components. Also, users tend to use *default* initial guesses that they have been familiar with to save time, which is an important source of subjectivity that could bias estimates. Egli (2003) and Maxbauer et al. (2016) run further optimizations with random distribution parameters that are resampled based on user-provided initial guesses. However, it is still subject to users' choice to some degree. The automated procedure for the choice of initial guesses (see section 2.1) could further improve the efficiency and objectivity of the analysis. The simplest strategy for automatic sampling is to randomly choose initial guesses from the parameter space, whereby the chance of getting to different minima of the object function becomes similar. Since the automated procedure is effortless for users, more combinations of initial guesses can be easily tested and therefore helpful to increase the chance of reaching the global minimum. It is possible to optimize the strategy for automatically choosing initial guesses in order to further increase the chance of reaching the global minimum. Unfortunately, in the presence of noise, the global minimum does not necessarily correspond to the correct solution even if the model distribution is identical to the coercivity distribution of the underlying magnetic component (see section 3.3 and Figure 5c as an example). Noise reduction will be discussed in section 4.4.

As mentioned above, noise further complicates the problem of nonuniqueness. Noise may change the position of local and global minima, and therefore, the result of component analysis may vary with noise, as demonstrated in Figure 4. It is therefore important to verify if results based on a given model distribution are consistent. One practical way to assess the consistency is to perform the analysis on independent measurements or on subsets of data generated by resampling (Egli, 2003; Maxbauer et al., 2016). The original data should have a sufficient number of data points ($n \geq 30$ is recommended) in the interval where the slope of acquisition curves is nonzero so that resampling can generate more effective subsets where the fraction of repeated data points between any two subsets is minor while including enough data points in subsets. Comparing results derived by the CDF and PDF forms of mixture models provides an additional check on the consistency of results. This is because, as shown in Figures 4b and 4d, raw data and gradient curves have different noise levels; therefore, they can be treated as independent measurements in terms of noise.

4.3. Residuals Due to Model Difference

Apart from noise, residual can arise from the fact that the model distribution is different from coercivity distributions of actual components. As shown in Figure 2, the residual is comparable to the magnitude of noise in real measurements (Figure 6d). Unlike measurement noise, residuals of this kind are sinusoidal. Though such residuals can be effectively reduced by using more components, resulting analyses would not have proper physical meanings. Statistics such as the AIC score may also overestimate the optimal number of components. For example, as in the case shown in Figure 2, the AIC score would suggest that two or three components are optimal, while there is only one actual component. Therefore, it is important to be aware that better statistics and smaller residuals do not necessarily imply that the corresponding results are physically justified. Alternatively, the AIC score should be considered as an upper limit of the actual number of components of the sample. In order to tell if data are over-fitted, it is insightful to compare the results derived from different model distributions, as shown in Figures 6 and 7. If the results are inconsistent, they are likely spurious, implying fewer components should be considered. This consideration is recommended especially when minor components (i.e., those with concentration of a few percent) are present. It is also helpful to compare results derived from similar samples to examine if identified components are consistent.

4.4. Noise Reduction

As illustrated above, the component analysis is in general sensitive to noise for all model distributions. Unfortunately, the signal-to-noise ratio of ordinary measurements is unlikely to guarantee unambiguous analyses especially for sediments and other weakly magnetized samples. The level of measurement noise shown

in Figure 6 would be considered as common in practice. However, it is high enough to bias component analysis as suggested by modeled data (Figures 4 and 5). Therefore, noise reduction is often desired before the analysis. The common ways of reducing noise are to smooth data using the cubic spline (Heslop et al., 2002; Maxbauer et al., 2016) or filtering (Egli, 2003). Cubic spline smoothing is a universal method; however, it is often arbitrary to choose the smoothing factor which affects how well the noise is separated from the signal. With small smoothing factors, the data will remain too noisy for component analysis. On the other hand, too much smoothing would remove more signal from data. Another choice is to filter the data. Simple low-pass filtering does not work as the frequency domain of white noise overlaps with that of the signal. Instead of filtering raw data, Egli (2003) applies filtering to residuals that are derived from a tailored linearization approach. This specialized method depends on the goodness of linearization and the choice of cutoff frequency, which is not always clear for users to determine. For example, based on our numerical experiments, the residuals between the modeled noise and estimated noise have a dominant low-frequency component (e.g., blue lines in Figures 4b, 4d, 4e, and 4h and 5b and 5d). If this residual could be removed from data, component analysis would land on the correct estimate more likely. However, as the frequency of these minor residuals varies case by case and it overlaps with the low-frequency component of signals, it is difficult to achieve this goal by choosing an optimal cutoff frequency for filtering. Therefore, even the tailored filtering process could not separate the noise efficiently. In fact, it is ambitious to expect the noise can be removed precisely especially given the fact that noise is not the only source of residuals (see section 4.3).

The practical purpose of noise reduction should be smoothing sharp variations due to noise, which are of high frequency. We suggest that overfitting can be used as a straightforward and efficient method to smooth data. In general, the residual becomes smaller as the number of components (n_c) increases. When n_c is insufficient, a significant fraction of signal cannot be approximated by the fit. In contrast, overfitting can approximate the signal and even some small features due to noise, whereby more information of noise is kept compared to the fitting with the optimal number of components suggested by the AIC score. Furthermore, as the shape of the overfitted curve is restricted by the mixture model, it is impossible to trace the random variations of noise. Therefore, the high-frequency noise is lost after overfitting. For the purpose of data smoothing, the constraints on the parameters of components mentioned in 2.1 should be relaxed. For example, the contribution can be negative and the shape can be arbitrary. In addition, as the overfitted curve is essentially a combination of components of the model distribution used for smoothing, subsequent component analysis should use different model distributions in order to minimize the dependence of component analysis on data smoothing. In this sense, the SGG and Burr type XII distributions are complementary.

In addition to data processing, the users should strive to obtain high-quality data. Paterson et al. (2018) summarized a series of strategies that can optimize hysteresis measurements, which also applies to the measurement of remanent magnetization. For example, increasing the averaging time at each measurement point is an effective way to improve the signal-to-noise ratio. When necessary, multiple ($n > 3$) measurements of a single sample should be measured and stacked to effectively suppress noise.

5. Conclusions

The component analysis of remanent magnetization curves is an important rock magnetic method to separate magnetic mixtures in natural samples. The model distribution that approximates the coercivity distribution of the magnetic component plays a fundamental role. However, the choice of model distributions is limited and remains empirical due to the lack of experimental and theoretical constraints on coercivity distributions of end-member components. In this study, the Burr type XII distribution is tested as a model distribution and compared with existing model distributions. Characteristic samples are used as end-member components to test different model distributions. It is found that the Burr type XII and SGG distributions can closely fit the experimental data with a single component while the lognormal component is associated with larger residuals especially in the lower end of the coercivity distribution. As the number of components increases, component analysis often has nonunique solutions, causing uncertainty in results. With modeled data, it is illustrated using the Burr type XII and SGG distributions that results are affected by the choice of initial guesses for parameters of individual components and measurement noise. To optimize the procedure for choosing initial guesses, an automatic protocol is designed to run multiple analyses with different sets of initial values that are randomly sampled from the parameter space. The solution with the smallest RSS among

the results is determined as the optimal solution. This procedure improves the efficiency and objectivity of component analysis. Measurement noise plays a detrimental role in component analysis; however, it is challenging to remove noise from data. Therefore, it is critical to obtain high-quality data, and it is recommended to use the cumulative form of the mixture model to fit raw data in order to avoid the amplification of noise by taking the derivative of raw data. Nevertheless, comparison between the analyses of raw data and derivatives is helpful to assess the uncertainty associated with the results. Despite the nonuniqueness of results, estimated components may be irrelevant with the actual physical components in analyzed samples. Therefore, further efforts are necessary to verify the reliability of results. We demonstrated using experimental data that it is useful to compare the results derived from different model distributions. Consistency among results is considered as a supportive evidence for a reliable interpretation of constituent components. In contrast, if the results are highly sensitive to the choice of model distributions, it would indicate either that key parameters (such as the number of components) involved in the analysis are questionable or that at least some of the selected model distributions are inappropriate. In order to better understand the suitability of each model distribution, it is recommended to investigate more end-member magnetic components in future studies.

Acknowledgments

We would like to thank Yongxin Pan, Chunsheng Jin, and Zhifeng Liu for providing data and Takayuki Kawashima for helpful discussion. We are grateful to Christoph Geiss and Daniel Maxbauer for their constructive reviews that significantly improved our manuscript. This work was supported by NIPR through an Advanced Project (KP-7 and KP301) and JSPS KAKENHI grants (15K13581, 16H04068, 17H06321, and 18K13638). This study was also performed under the cooperative research program of the Center for Advanced Marine Core Research, Kochi University (14A037, 14B034, 15A047, and 15B042). Z. J. acknowledges Natural Science Foundation of China (grant 41504055). Experimental data that were analyzed and shown in this paper can be found in <https://sites.google.com/a/nipr.ac.jp/magz/>

References

- Akaike, H. (1998). Information theory and an extension of the maximum likelihood principle. In E. Parzen, K. Tanabe, & G. Kitagawa (Eds.), *Selected papers of Hirotugu Akaike, Springer Series in Statistics (Perspectives in Statistics)* (pp. 199–213). New York, NY: Springer. https://doi.org/10.1007/978-1-4612-1694-0_15
- Burnham, K. P., & Anderson, D. R. (2002). *Model selection and multimodel inference: A practical information-theoretic approach* (2nd ed.). New York: Springer-Verlag. <https://doi.org/10.1007/b97636>
- Burr, I. W. (1942). Cumulative frequency functions. *The Annals of Mathematical Statistics*, 13(2), 215–232. <https://doi.org/10.1214/aoms/1177731607>
- Egli, R. (2003). Analysis of the field dependence of remanent magnetization curves. *Journal of Geophysical Research*, 108(B2), 2081. <https://doi.org/10.1029/2002JB002023>
- Egli, R. (2004a). Characterization of individual rock magnetic components by analysis of remanence curves. 1. Unmixing natural sediments. *Studia Geophysica et Geodaetica*, 48(2), 391–446. <https://doi.org/10.1023/B:SGEG.0000020839.45304.6d>
- Egli, R. (2004b). Characterization of individual rock magnetic components by analysis of remanence curves. 2. Fundamental properties of coercivity distributions. *Physics and Chemistry of the Earth, Parts A/B/C*, 29(13–14), 851–867. <https://doi.org/10.1016/j.pce.2004.04.001>
- Egli, R. (2004c). Characterization of individual rock magnetic components by analysis of remanence curves. 3. Bacterial magnetite and natural processes in lakes. *Physics and Chemistry of the Earth, Parts A/B/C*, 29(13–14), 869–884. <https://doi.org/10.1016/j.pce.2004.03.010>
- Egli, R. (2009). Magnetic susceptibility measurements as a function of temperature and frequency I: Inversion theory. *Geophysical Journal International*, 177(2), 395–420. <https://doi.org/10.1111/j.1365-246X.2009.04081.x>
- Egli, R., Chen, A. P., Winklhofer, M., Kodama, K. P., & Horng, C. (2010). Detection of noninteracting single domain particles using first-order reversal curve diagrams. *Geochemistry, Geophysics, Geosystems*, 11, Q01Z11. <https://doi.org/10.1029/2009GC002916>
- Evans, M. E., & Heller, F. (2003). *Environmental magnetism: Principles and applications of enviromagnetics*. San Diego, CA: Academic Press.
- Fujii, M., Okino, K., Sato, H., Nakamura, K., Sato, T., & Yamazaki, T. (2016). Variation in magnetic properties of serpentinized peridotites exposed on the Yokonawa Rise, Central Indian Ridge: Insights into the role of magnetite in serpentinization. *Geochemistry, Geophysics, Geosystems*, 17, 5024–5035. <https://doi.org/10.1002/2016GC006511>
- Heslop, D. (2015). Numerical strategies for magnetic mineral unmixing. *Earth-Science Reviews*, 150, 256–284. <https://doi.org/10.1016/j.earscirev.2015.07.007>
- Heslop, D., Dekkers, M. J., Kruijver, P. P., & Van Oorschot, I. H. M. (2002). Analysis of isothermal remanent magnetization acquisition curves using the expectation-maximization algorithm. *Geophysical Journal International*, 148(1), 58–64. <https://doi.org/10.1046/j.0956-540x.2001.01558.x>
- Heslop, D., & Dillon, M. (2007). Unmixing magnetic remanence curves without a priori knowledge. *Geophysical Journal International*, 170(2), 556–566. <https://doi.org/10.1111/j.1365-246X.2007.03432.x>
- Heslop, D., McIntosh, G., & Dekkers, M. J. (2004). Using time- and temperature-dependent Preisach models to investigate the limitations of modelling isothermal remanent magnetization acquisition curves with cumulative log Gaussian functions. *Geophysical Journal International*, 157(1), 55–63. <https://doi.org/10.1111/j.1365-246X.2004.02155.x>
- Heslop, D., & Roberts, A. P. (2012). A method for unmixing magnetic hysteresis loops. *Journal of Geophysical Research*, 117, B03103. <https://doi.org/10.1029/2011JB008859>
- Jiang, Z., Liu, Q., Zhao, X., Roberts, A. P., Heslop, D., Barrón, V., & Torrent, J. (2016). Magnetism of Al-substituted magnetite reduced from Al-hematite. *Journal of Geophysical Research: Solid Earth*, 121, 4195–4210. <https://doi.org/10.1002/2016JB012863>
- Kruijver, P. P., Dekkers, M. J., & Heslop, D. (2001). Quantification of magnetic coercivity components by the analysis of acquisition curves of isothermal remanent magnetisation. *Earth and Planetary Science Letters*, 189(3–4), 269–276. [https://doi.org/10.1016/S0012-821X\(01\)00367-3](https://doi.org/10.1016/S0012-821X(01)00367-3)
- Liu, Q., Jackson, M., Yu, Y., Chen, F., Deng, C., & Zhu, R. (2004). Grain size distribution of pedogenic magnetic particles in Chinese loess/paleosols. *Geophysical Research Letters*, 31, L22603. <https://doi.org/10.1029/2004GL021090>
- Liu, Q., Roberts, A. P., Larrasoña, J. C., Banerjee, S. K., Guyodo, Y., Tauxe, L., & Oldfield, F. (2012). Environmental magnetism: Principles and applications. *Reviews of Geophysics*, 50, RG4002. <https://doi.org/10.1029/2012RG000393>
- Maxbauer, D. P., Feinberg, J. M., & Fox, D. L. (2016). MAX UNMix: A web application for unmixing magnetic coercivity distributions. *Computers & Geosciences*, 95, 140–145. <https://doi.org/10.1016/j.cageo.2016.07.009>
- Paterson, G., Zhao, X., Jackson, M., & Heslop, D. (2018). Measuring, processing, and analyzing hysteresis data. *Geochemistry, Geophysics, Geosystems*, 19, 1925–1945. <https://doi.org/10.1029/2018GC007620>

- Roberts, A. P., Pike, C. R., & Verosub, K. L. (2000). First-order reversal curve diagrams: A new tool for characterizing the magnetic properties of natural samples. *Journal of Geophysical Research*, 105(B12), 28,461–28,475. <https://doi.org/10.1029/2000JB900326>
- Robertson, D. J., & France, D. E. (1994). Discrimination of remanence-carrying minerals in mixtures, using isothermal remanent magnetisation acquisition curves. *Physics of the Earth and Planetary Interiors*, 82(3–4), 223–234. [https://doi.org/10.1016/0031-9201\(94\)90074-4](https://doi.org/10.1016/0031-9201(94)90074-4)
- Rodriguez, R. N. (1977). A guide to the Burr type XII distributions. *Biometrika*, 64(1), 129–134. <https://doi.org/10.1093/biomet/64.1.129>
- Tadikamalla, P. R. (1980). A look at the Burr and related distributions. *International Statistical Review/Revue Internationale de Statistique*, 48(3), 337–344. <https://doi.org/10.2307/1402945>
- von Dobeneck, T. (1996). A systematic analysis of natural magnetic mineral assemblages based on modelling hysteresis loops with coercivity-related hyperbolic basis functions. *Geophysical Journal International*, 124(3), 675–694. <https://doi.org/10.1111/j.1365-246X.1996.tb05632.x>
- Zhao, X., & Liu, Q. (2010). Effects of the grain size distribution on the temperature-dependent magnetic susceptibility of magnetite nanoparticles. *Science China Earth Sciences*, 53(7), 1071–1078. <https://doi.org/10.1007/s11430-010-4015-y>